Supporting Information for

Vibrational Energy Transfer of Excited CO Molecules on NaCl(100): A Non-Equilibrium *Ab Initio* Molecular Dynamics Study

Shreya Sinha* and Peter Saalfrank*

Theoretical Chemistry, Institute of Chemistry, University of Potsdam, Karl-Liebknecht-Str. 24-25, 14476 Potsdam, Germany

E-mail: shreya.sinha@uni-potsdam.de; peter.saalfrank@uni-potsdam.de

Phone: +49 (0)331–977–5232

Contents

S1 AIMD calculations: Workflow

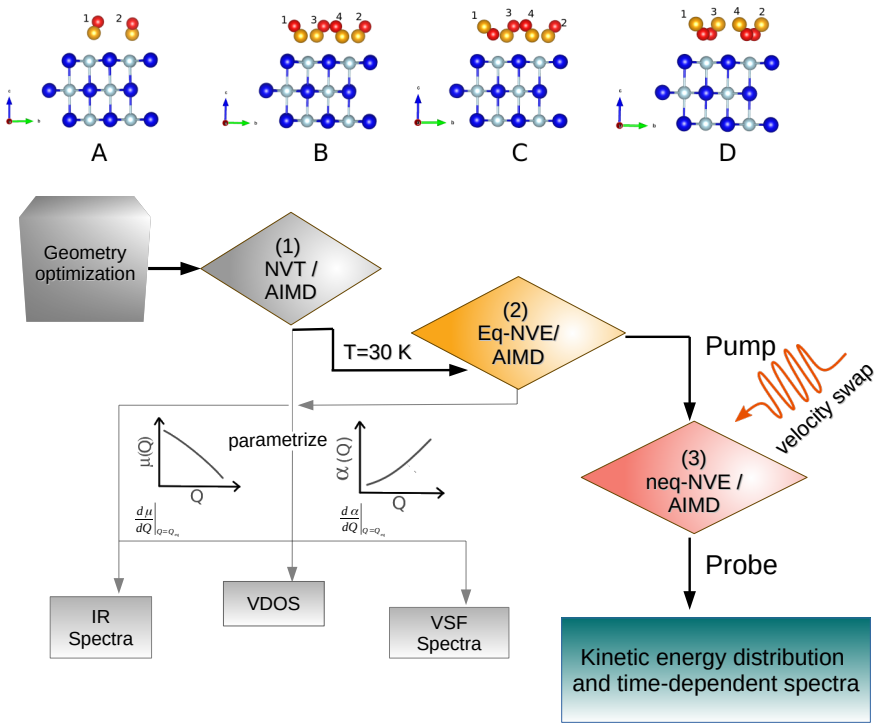

Figure S1: Schematic representation of the AIMD approach, applied to models A-D considered in this work. Optimized configurations are propagated in phase (1) in a canonical ("NVT") ensemble and equilibrated with a fixed temperature $T = 30$ K (using a Nosé Hoover thermostat), which are then propagated in phase (2) in the microcanonical ensemble ("Eq-NVE") to remove thermostat effect. In a phase (3), the action of a pump IR pulse is simulated *via* a velocity swapping approach by which we perturb the velocities of the selected atoms along selected normal modes (see Sec. S2). Then, each of these configurations are propagated with the determined velocities in the microcanonical ensemble (also phase 3, "neq-NVE") for a total of 10-20 ps (3-6 trajectories each) in most of the cases amounting to a total of 30-120 ps respectively. The optimized configurations (models) used for the study is highlighted in the upper panel. The greyscale boxes represent evaluation of equilibrium spectra and vibrational features, *e.g.* IR spectra (which require a parametrization of the dipole function), the VDOS, and VSF spectra (which require a parametrization also of the polarizability). Details are described in Ref.[1] In the present work, only VDOS and VSF spectra are considered, albeit in a time-dependent manner. In addition, in phase (3) atom-resolved kinetic energies and other properties are computed.

S2 Velocity swapping approach

S2.1 Pumping energy into the CO internal stretch mode

We model excitation of the CO bond by utilizing the sudden velocity swapping procedure described by Jeon *et al*,[2] which has been previously implemented also for a different system (water on alumina) by Melani *et al.*[3] Here, we perturb the velocities of the oxygen and carbon of an adsorbed CO molecule such that the bond kinetic energy increases by $n\hbar\omega_{vib}$ where $n = 1, 2$ for instance. This models the vibrational excitation of the CO stretch to 1st and 2nd excited state, respectively, within a classical MD context. The perturbation is done along the CO bond vector direction. Under these conditions, the perturbed velocities are given, in terms of unperturbed velocities, as:

$$
\begin{aligned}
&\underline{v}_{\mathrm{O}} = \underline{v}^0_{\mathrm{O}} + \epsilon_{\mathrm{O}}\ \hat{\underline{r}}_0, \qquad \underline{v}_{\mathrm{C}} = \underline{v}^0_{\mathrm{C}} + \epsilon_{\mathrm{C}}\hat{\underline{r}}_0 \\
&\epsilon_{\mathrm{O}} = \frac{(p - p_0)}{m_{\mathrm{O}}}, \qquad \epsilon_{\mathrm{C}} = -\frac{(p - p_0)}{m_{\mathrm{C}}} \\
&p = \frac{p_0}{|p_0|}(p_0^2 + 2\ \mu\ \nu_{\mathrm{stretch}}\ \hbar\omega_{vib})^{1/2}, \qquad p_0 = \mu(\underline{v}^0_{\mathrm{O}} - \underline{v}^0_{\mathrm{C}}) \cdot \hat{\underline{r}}_0 \\
&\hat{\underline{r}}_0 = \frac{(x_{\mathrm{O}} - x_{\mathrm{C}})\hat{\underline{x}} + (y_{\mathrm{O}} - y_{\mathrm{C}})\hat{\underline{y}} + (z_{\mathrm{O}} - z_{\mathrm{C}})\hat{\underline{z}}}{\sqrt{(x_{\mathrm{O}} - x_{\mathrm{C}})^2 + (y_{\mathrm{O}} - y_{\mathrm{C}})^2 + (z_{\mathrm{O}} - z_{\mathrm{C}})^2}}
\end{aligned}
$$

Here, $\hat{\underline{r}}_0$ is the unit vector parallel to $\underline{r}_{\mathrm{O}} - \underline{r}_{\mathrm{C}}$, $\underline{v}^0_{\mathrm{C}}$ and $\underline{v}^0_{\mathrm{O}}$ are the unperturbed velocities, ω_{vib} ($=\omega^{\mathrm{stretch}}_{\mathrm{CO}}$) is the CO internal stretch vibrational energy (~ 0.26 eV ≈ 2100 cm^{-1}). $\hat{\underline{x}}$, $\hat{\underline{y}}$, $\hat{\underline{z}}$ are Cartesian unit vectors; p_0, p are unperturbed and perturbed momenta multiplied by $\hat{\underline{r}}_0$, μ is the reduced mass of CO, $(m_{\mathrm{C}}m_{\mathrm{O}}/(m_{\mathrm{C}} + m_{\mathrm{O}}) \sim 6.857$ amu) and ϵ_{C}, ϵ_{O}, are the velocity scaling factors. For a schematic illustration, see Fig. S2(a).

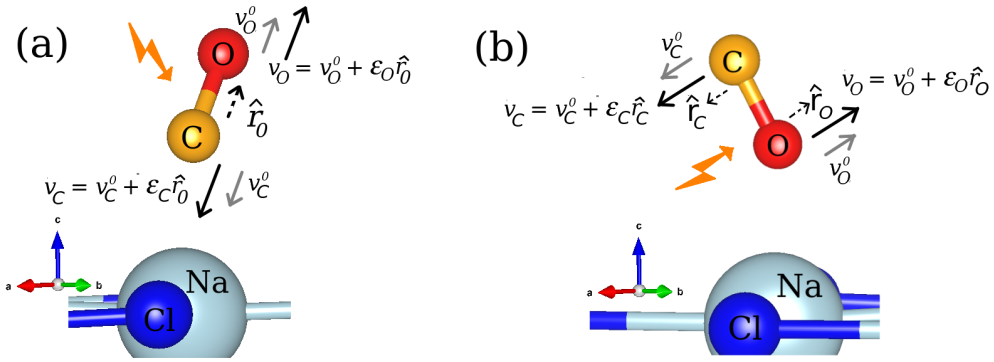

Figure S2: Schematic representation of the velocity swap approach utilized here to pre-excite the (a) C-O stretch mode (b) frustrated bending mode in our CO/NaCl(100) system .

S2.2 Pumping energy into a CO frustrated bending mode

We model a direct excitation of the low frequency (LF) librational modes to higher vibrational levels. Herein, we pump energy into an n-fold vibrationally excited frustrated bending mode (also called rotational mode in this work), chosen from a normal mode analysis of an isolated CO on NaCl(100) (see Tab. S1). The magnitude of chosen excess energy is 0.26 eV ($\sim$ 2100 cm^{-1}) such that the energy of the n^{th} vibrational excitation nearly overlaps with $\nu_{\text{stretch}} = 1$ of the CO molecule. Note that this energy is above the classical isomerization barrier for "C-down" $\leftrightarrow$ "O-down" isomerization (574 cm^{-1} w.r.t. "O-bound" and 1200 cm^{-1} w.r.t. "C-bound" geometry) for a 1/4 ML CO/NaCl(100) and also for monolayer CO/NaCl(100). Therefore, this energy suffices to also invert CO molecules on NaCl. A schematic representation of the velocity swapping method for the frustrated rotation is shown in Fig. S2 (b) and is as follows:

$$\underline{v}_{\text{O}} = \underline{v}^0_{\text{O}} + \epsilon_{\text{O}}\underline{\hat{r}}_{\text{O}}, \qquad \underline{v}_{\text{C}} = \underline{v}^0_{\text{C}} + \epsilon_{\text{C}}\underline{\hat{r}}_{\text{C}}$$

$$\epsilon_{\text{O}} = \frac{|(p - p_0)|}{m_{\text{O}}}, \qquad \epsilon_{\text{C}} = \frac{|(p - p_0)|}{m_{\text{C}}}$$

$$p = \frac{p_0}{|p_0|}(p_0^2 + 2\mu\ \nu_{\text{bend}}\ \hbar\omega_{vib})^{1/2}, \qquad p_0 = \mu(\underline{v}^0_{\text{O}} - \underline{v}^0_{\text{C}}) \cdot \underline{\hat{r}}_{\text{eff}}$$

$$\underline{\hat{r}}_{\text{eff}} = \frac{(dx_{\text{O}} + dx_{\text{C}})\underline{\hat{x}} + (dy_{\text{O}} + dy_{\text{C}})\underline{\hat{y}} + (dz_{\text{O}} + dz_{\text{C}})\underline{\hat{z}}}{\sqrt{(dx_{\text{O}} + dx_{\text{C}})^2 + (dy_{\text{O}} + dy_{\text{C}})^2 + (dz_{\text{O}} + dz_{\text{C}})^2}}$$

$$\hat{\underline{r}}_l = dx_{(l)}\hat{\underline{x}} + dy_{(l)}\hat{\underline{y}} + dz_{(l)}\hat{\underline{z}} \quad l \in [\mathrm{O}, \mathrm{C}]$$

The normalized eigenvector components, $dx_{(l)}$, $dy_{(l)}$ and $dz_{(l)}$ of the l^{th} atom , $l \in$ [C, O], for a "C-bound" and "O-bound" CO atop NaCl(100), computed for a 0.25 ML CO on NaCl(100) modelled by a $2\sqrt{2}\times 2\sqrt{2}\times 3$ unit cell at the PBE+D2 level of theory, are reported in Tab.S1.

An alternative method involves distributing the total energy in a mass-weighted manner such that excess energy is injected into individual C and O atoms, achieving the desired mode excitation:

$$\begin{aligned}
\underline{v}_{\mathrm{O}} &= \underline{v}^0_{\mathrm{O}} + \epsilon_{\mathrm{O}}\hat{\underline{r}}_{\mathrm{O}}, \quad \underline{v}_{\mathrm{C}} = \underline{v}^0_{\mathrm{C}} + \epsilon_{\mathrm{C}}\hat{\underline{r}}_{\mathrm{C}} \\
\epsilon_{\mathrm{O}} &= \frac{|(p^{(\mathrm{O})} - p_0^{(\mathrm{O})})|}{m_{\mathrm{O}}}, \quad \epsilon_{\mathrm{C}} = \frac{|(p^{(\mathrm{C})} - p_0^{(\mathrm{C})})|}{m_{\mathrm{C}}} \\
p^{(l)} &= \frac{p_0^{(l)}}{|p_0^{(l)}|}(p_0^{(l)2} + 2m_l\Delta E_l)^{1/2}, \quad p_0^{(l)} = m_l \underline{v}^0_{(l)} \cdot \hat{\underline{r}}_l, \\
p_0^{(l)} &= p_0^{(l)x} + p_0^{(l)y} + p_0^{(l)z}, \\
\hat{\underline{r}}_l &= (dx)_{(l)}\hat{\underline{x}} + (dy)_{(l)}\hat{\underline{y}} + (dz)_{(l)}\hat{\underline{z}} \\
\Delta E_l &= \frac{m_l}{\sum_l m_l}\nu_{\text{bend}}\hbar\omega_{vib}, \quad l \in [\mathrm{O}, \mathrm{C}]
\end{aligned}$$

Here, ΔE_l are the respective mass-weighted energies. Both methods yield similar results, so we combine the succeeding microcanonical trajectories simulated using both, and report averaged results (from six trajectories).

Table S1: Normalized eigenvector components (in Å) of a bending mode in a "C-bound" CO (152.94 cm^{-1}, 18.96 meV) and "O-bound" CO (80.57 cm^{-1}, 9.98 meV) for a 0.25 ML CO on NaCl(100) modelled by a $2\sqrt{2} \times 2\sqrt{2} \times 3$ unit cell at the PBE+D2 level of theory, see Fig. 1(a) in Ref.[1] Only adsorbate atoms were displaced for the evaluation of normal modes.

atom type	bending "C-bound"			"O-bound"		
	dx	dy	dz	dx	dy	dz
C	0.1591	0.9871	0.0169	-0.9371	0.2073	0.2809
O	-0.1695	-0.9853	0.0201	0.9646	-0.2069	0.1633

S3 Normalization of VDOS

The ΔVDOS curves of the individual subsystems shown in this work and defined in Eq.(4) of the main text, are normalized w.r.t. the total ΔVDOS at every Δt. The time window as well as the normalization factor always impacts the spectral profile shapes to some extent. For instance, in the internal mode picture, we always calculate vibrational density of states considering only the velocities of the internal degrees of freedom of the carbon and oxygen atoms which accentuates the dynamics of the vibrational modes of the CO adsorbates and is reflected in the ΔVDOS curves compared to Cartesian ΔVDOS curves, where the movable surface atoms are also included in the total VDOS.

S4 Angular distribution probabilities

Angular distribution probabilities (%) are evaluated as: $P(\theta) = n_\theta/N_t \times 100\%$ and $P(\phi) = n_\phi/N_t \times 100\%$, where n_θ and n_ϕ are the number of timesteps associated with a certain value of θ and ϕ, the latter discretized by a binning system, and N_t is the total number of timesteps. Joint probability distributions, $P(\theta, \phi)$, can be therefore computed as: $P(\theta, \phi) = n_{\theta,\phi}/N_t \times 100\%$ where $n_{\theta,\phi}$ is now the number of timesteps associated with a certain tuple $\{\theta, \phi\}$. A bin width of 10° is chosen for θ and ϕ in this work.

S5 Vibrational relaxation of $\nu_{\mathbf{stretch}} = 1$ in monolayer CO/NaCl(100)

In the main text, Sec. 3.1.1 among other things, the excitation of all four CO molecules in "all C-down" monolayer CO/NaCl(100) (model B) was considered, and the subsequent dynamics. Here additional information is given for that scenario.

Besides Fig. S3, which shows molecule-resolved VDOS curves, we also provide an in-

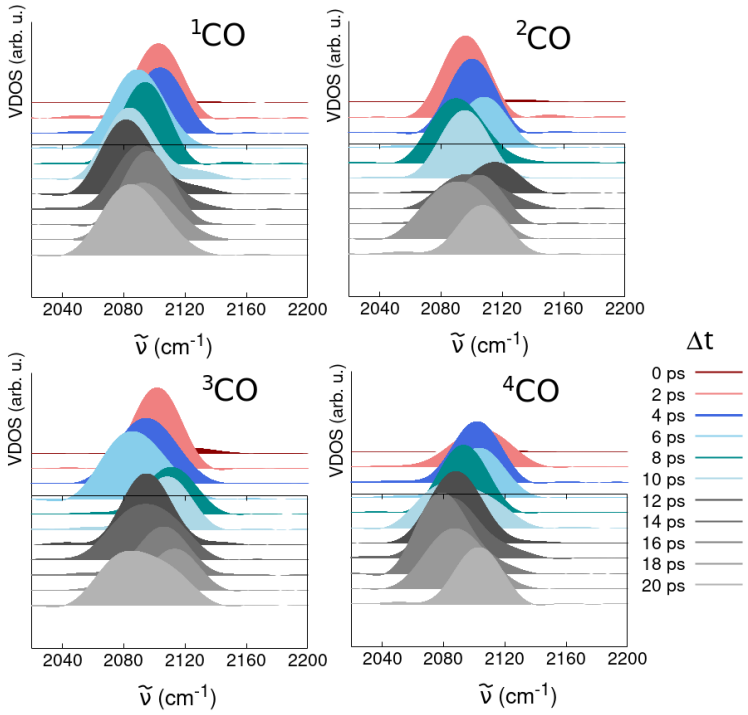

Figure S3: Molecule-resolved time-dependent VDOS in the $\nu_{\text{stretch}} = 1$ region of 1 ML all "C-bound" CO/NaCl(100), where all CO adsorbates are pre-excited by one vibrational quantum. $\Delta t = 0$ indicates the time of pre-excitation.

tramolecular mode-resolved analysis of the integrated ΔVDOS curves for this case, which provides lifetimes / rates for energy exchange between various subsystems. We report in Fig. S4 the mode-resolved difference integrated VDOS contribution from each CO adsorbate, normalized by the total integrated VDOS of the respective CO adsorbate(s) (this excludes contributions from the NaCl surface). The ΔVDOS is mode-resolved by integration according to Eq. (4) in the main text, using limits $[\omega_1, \omega_2]$ = [2050, 2200] cm^{-1} for the CO internal stretch mode, ν_{stretch}=1, [4050, 4280] cm^{-1} for ν_{stretch}=2, and [0, 300] cm^{-1} for the low frequency librational modes. In Fig. S4, an exponential decay and growth is observed in the ΔVDOS curves the CO stretch region ν_{stretch}=1 and librational modes respectively, for the individual CO adsorbates. Performing exponential fits for these modes for molecule ^{1}CO (inset), yields relaxation times of 3 ps for the decaying CO stretch mode, and a characteristic time of 1.23 ps for the librational, energy-accepting modes. This indicates that the transient changes in the ΔVDOS within the same molecule returns back to its equilibrium state within a few picoseconds.

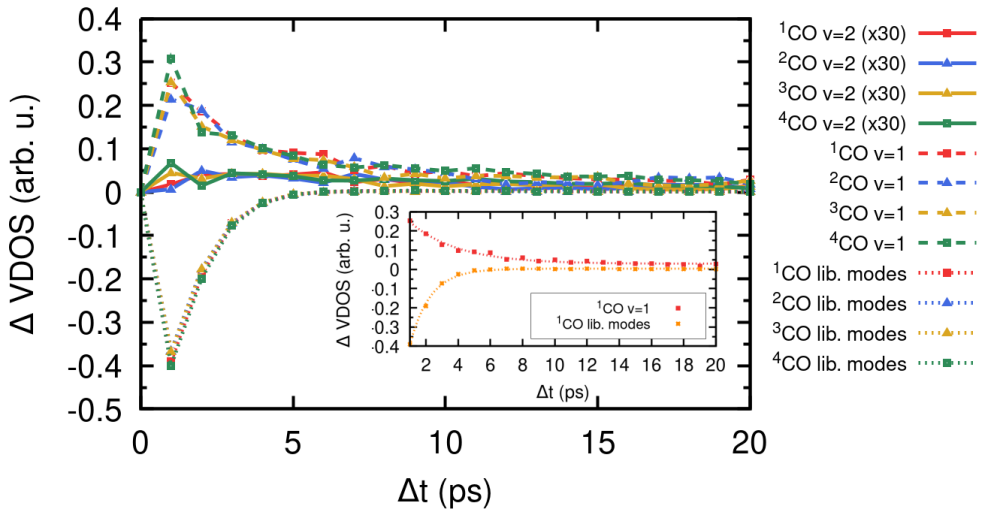

Figure S4: Integrated VDOS curves decomposed into specific frequency fingerprint regions, where the molecular VDOS for the individual CO adsorbates are normalized for the case where the CO stretch mode of all the four CO molecules are pre-excited by one vibrational quantum each. The inset gives an exponential fit for the relaxation of stretch and librational modes for ^{1}CO.

From Fig. S4 already some small participation of VDOS in the $\nu_{\text{stretch}} = 2$ frequency region for all the CO adsorbates can be anticipated. In fact a $\nu_{\text{stretch}} = 2$ peak appears for all CO adsorbates, showcasing broadened double-peaked progressions, the proportion of the red-shifted progression corresponding to the proportion of vibrationally heating in the respective subsystem (*cf.* Fig. S5).

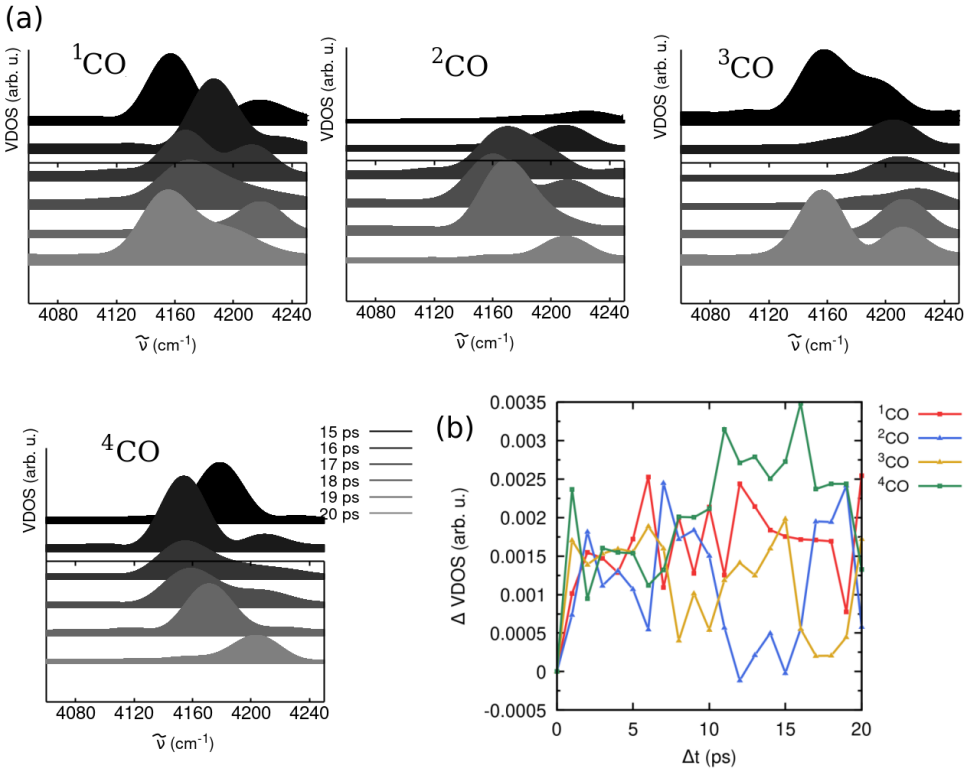

Figure S5: (a) Time-dependent VDOS (in the last 5 ps of simulations), and (b) integrated ΔVDOS in the $\nu_{\text{stretch}} = 2$ CO stretch region for the CO adsorbates. Excitation was done at 5 ps.

S6 Vibrational relaxation of $\nu_{\mathbf{stretch}} = 1$ in monolayer all "O-bound" CO/NaCl(100)

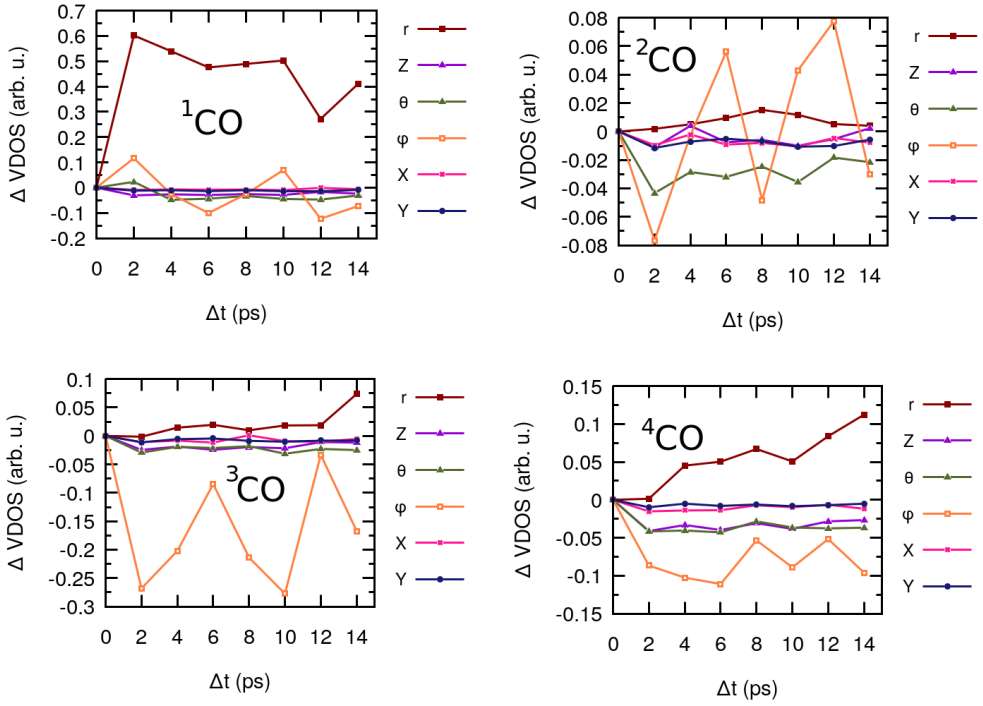

Figure S6: Integrated change of the decomposed internal VDOS for all four CO molecules after pre-excitation of the CO stretch mode of an "O-bound" CO in an all "O-bound" monolayer of CO/NaCl(100) (model D) by 0.26 eV.

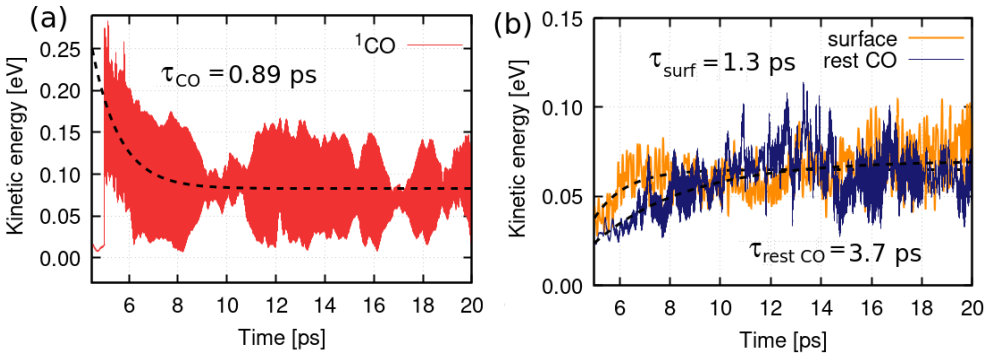

Figure S7: Exponential fits and extracted relaxation times of the averaged instantaneous kinetic energy curves of (a) the pre-excited "O-bound" CO, ^{1}CO, and (b) the NaCl surface and the neighbouring CO adsorbates in a monolayer CO/NaCl(100), when excess energy equivalent to 0.26 eV is pumped into the CO stretch mode of an "O-bound" CO surrounded by "O-bound" neighbours (model D). The fit function for an energy-loosing subsystem is given by Eq.(1) of the main text. Further, the fits done for the two accepting subsystems, were done with Eq.(2) of the main text. In both panels, excitation occurs at 5 ps.

S7 Vibrational relaxation of $\nu_{\mathbf{bend}} = 26$ in monolayer CO/NaCl(100)

The integrated internal ΔVDOS curves shown in Fig. S8 offer further microscopic insight into the VET dynamics. For instance, the excess energy gets pumped into the ϕ DoF of the targeted molecule, part of which gets transferred to the CO stretch DoF (r) within a sub-picosecond time interval. This eventually gets inter/intra-molecularly redistributed to other internal DoFs. Specifically, the azimuthal DoF excitation is redistributed *via* (ϕ, ϕ) coupling to the azimuthal DoF and other librational modes (predominantly θ, Z) of the neighbouring CO adsorbates. The rate of this energy transfer is again faster compared to the V-V transfer along the stretch mode. The integrated Cartesian ΔVDOS is also reported in Fig. S9.

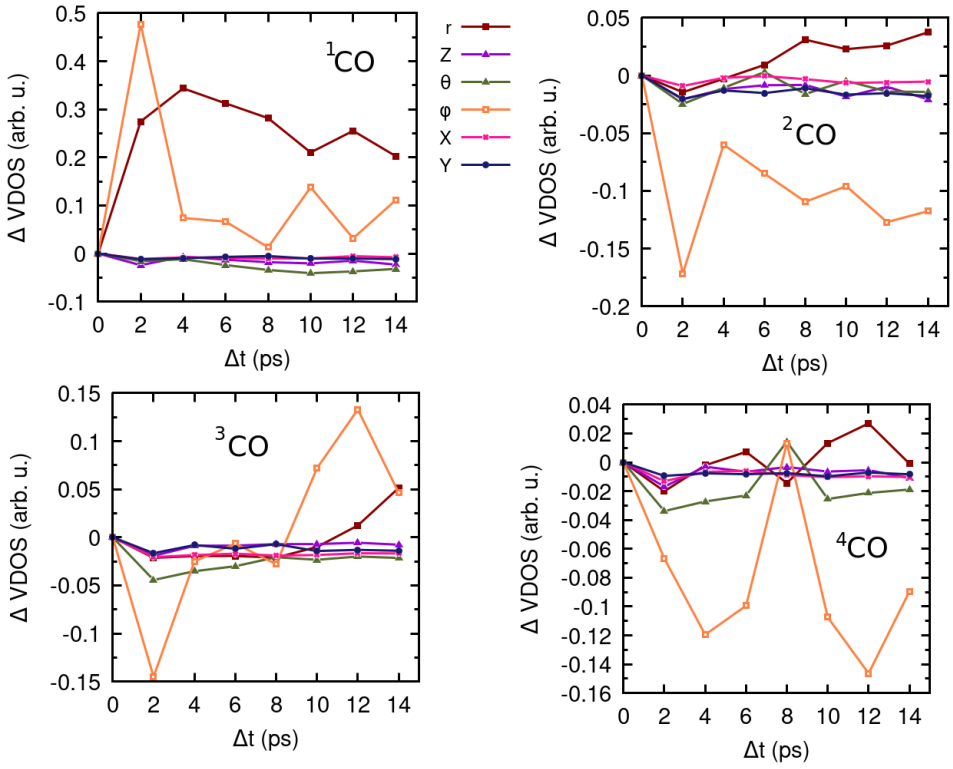

Figure S8: Integrated change of the decomposed internal VDOS for all four CO molecules after pre-excitation of a bending mode of one "O-bound" CO by $\sim$ 26 vibrational quanta (0.26 eV) in a monolayer one "O-bound" CO/NaCl(100) (model C).

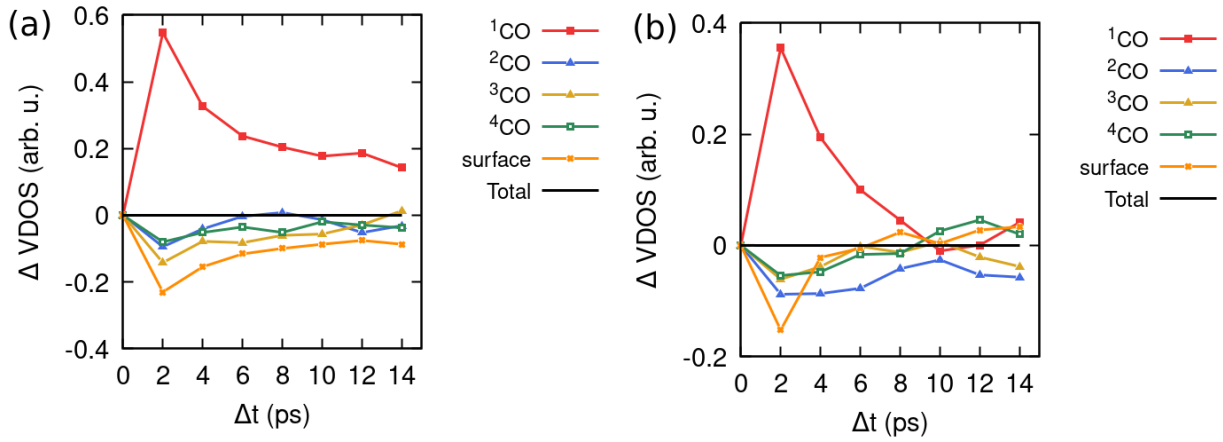

Figure S9: (a) Integrated change of Cartesian ΔVDOS after pre-excitation of a bending mode by 0.26 eV of an (a) "O-bound" (model C) and (b) "C-bound" CO (model B) in a monolayer CO/NaCl(100).

S8 Vibrational relaxation lifetimes for frustrated-rotation excited models

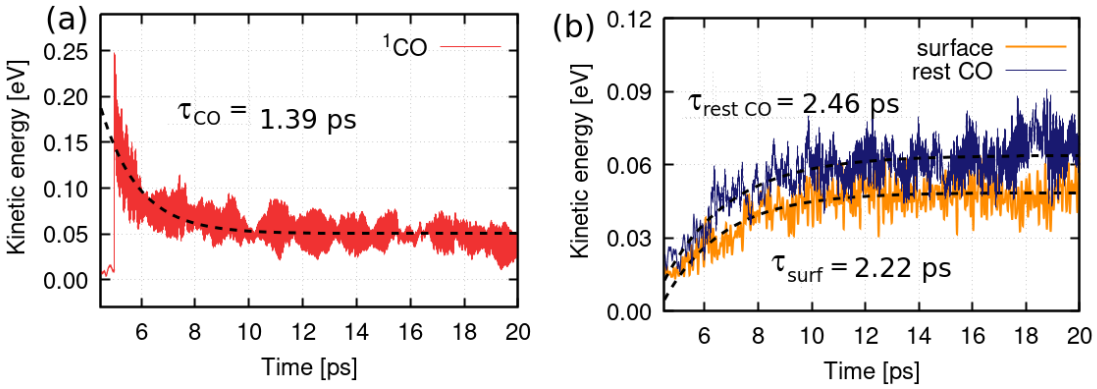

Figure S10: Exponential fits and extracted relaxation times of the averaged instantaneous kinetic energy curves of (a) the pre-excited "O-bound" CO, and (b) the surface and the neighbouring CO adsorbates in a monolayer CO/NaCl(100) with neighbours "C-down" (model C), when excess energy equivalent to 0.26 eV is pumped into a frustrated rotational mode. The fit function for an energy-loosing subsystem is given by Eq.(1) of the main text. Further, the fits done for the two accepting subsystems, were done with Eq.(2) of the main text. Excitation was done at 5 ps.

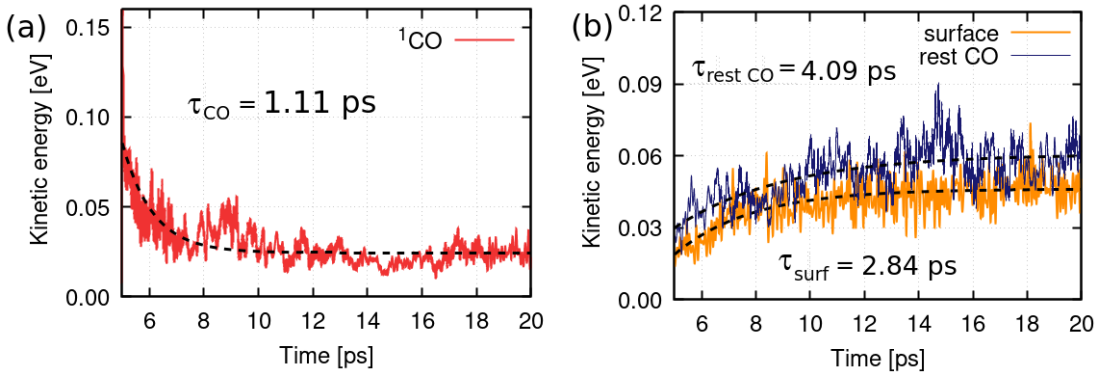

Figure S11: Exponential fits and extracted relaxation times of the averaged instantaneous kinetic energy curves of (a) the pre-excited "C-bound" CO, and (b) the surface and the neighbouring CO adsorbates in a monolayer CO/NaCl(100) with neighbours "C-down" (model B), when excess energy equivalent to 0.26 eV is pumped into a frustrated rotational mode. The fit function for an energy-loosing subsystem is given by Eq.(1) of the main text. Further, the fits done for the two accepting subsystems, were done with Eq.(2) of the main text. Excitation was done at 5 ps.

S9 Time-dependent non-linear correlations

Here, we present a brief discussion on the time-dependent distance correlation matrices evaluated for the CO adsorbates for a few scenarios namely (i) pre-excitation of the CO stretch mode by one vibrational quantum in an all "O-bound" monolayer (model D), (ii) a relaxing "O-down" CO in a one "O-bound" monolayer (model C) following pre-excitation in frustrated bending mode ($\nu_{\text{bend}} = 26$).

For case (i), in Fig. S12, we observe a decrease in correlation along the CO stretch mode for the pre-excited molecule with its neighbours, $(r_{^1\text{CO}}, r)$; this is reflected also in the internal ΔVDOS curves (see Fig. S6). This indicates a slow transfer of energy along the CO stretch mode (VV transfer) among the CO adsorbates. Conversely, correlations between the librational modes of the pre-excited molecule increase with the r mode of the neighbours, opening vibrational non-adiabatic channels of energy transfer between the low-frequency (LF) librational modes and the high-frequency (HF) CO stretch mode, also known as VT transfer. Also, angular and other LF mode intra-correlations increase during the course of simulations. For molecules adsorbed parallel w.r.t. the surface, relatively non-negligible intra-molecular correlations (in the range [0.2, 0.3]) between r and librational modes are found to decrease significantly (< 0.05) after pre-excitation of the neighbouring CO (not shown).

In case (ii), the time-dependent difference distance correlation matrices (not shown) illustrate a decrease in correlation between the HF CO stretch mode, r, and LF librational modes for the pre-excited molecule, complemented by an increase in correlation between the low frequency modes (predominantly between Z and θ). As for the neighbouring CO(s), $(r,\ r)$ correlations promote VV transfer and HF-LF intermolecular correlations are likely to promote VT transfer.

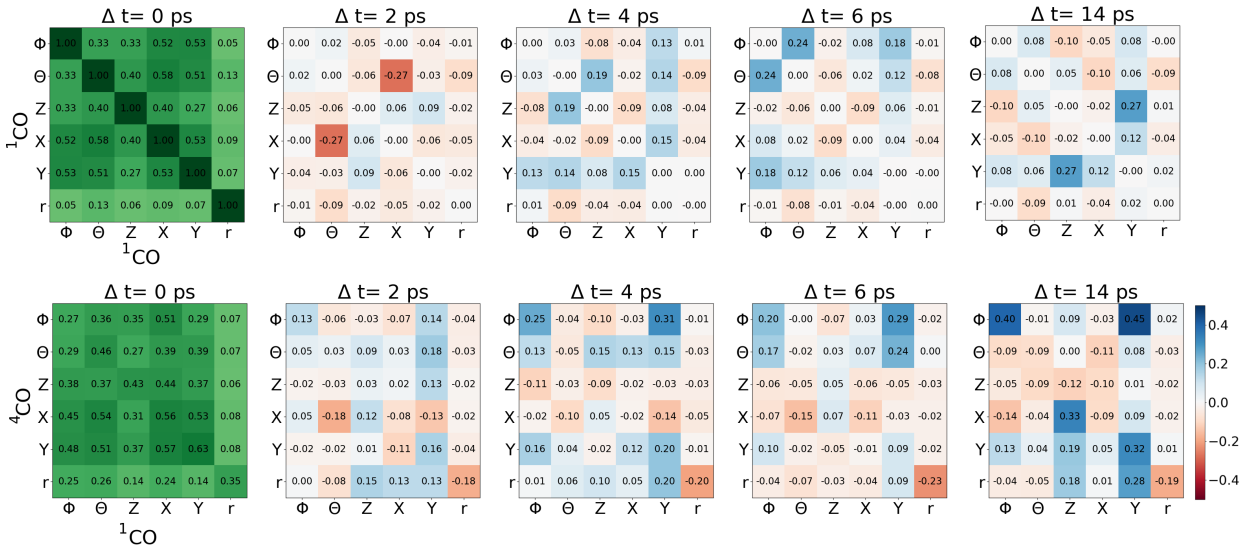

Figure S12: Time-dependent (difference) distance intra-correlation (upper panel) and inter-correlation (lower panel) matrices (see Eq. (6) in main text), over a 2 ps window, for Δt = 2, 4, 6, 14 ps during the course of the neq-AIMD simulations, averaged over 3 trajectories, when the CO stretch mode of an "O-bound" CO in an all "O-bound" 1 ML CO/NaCl(100) is pre-excited by one vibrational quantum (model D). At $\Delta t = 0$, the inter/intra- distance correlation matrix for the equilibrium scenario is reported.

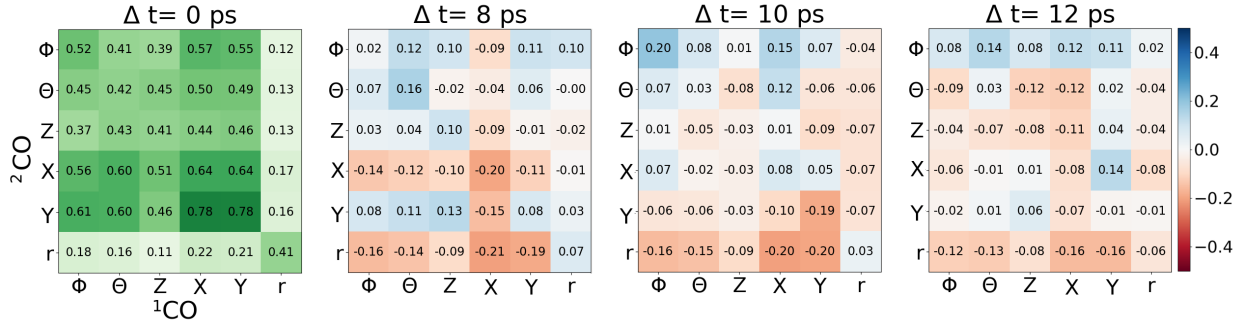

Figure S13: Time-dependent difference inter-distance correlation matrices (see Eq. (6) in main text), over a 2 ps window, Δt = 2, 8, 10, 12 ps during the course of the neq-AIMD simulations, averaged over 3 trajectories, when the CO stretch mode of one CO molecule in a 0.5 ML CO/NaCl(100) is pre-excited by 1 vibrational quantum; at $\Delta t = 0$, the inter-distance correlation matrix for the equilibrium scenario is reported.

S10 Analysis of non-equilibrium trajectories

Here we report averaged CO-surface (Z) distances, lateral displacements for CO adsorbates for cases where (1) an internal CO stretch mode of an "O-bound" adsorbate in an all "O-bound" monolayer is pre-excited by one vibrational quantum (model D, 0.26 eV excitation energy), a frustrated bending mode of (2) an "O-bound" CO in a one "O-bound" monolayer (model C), and a (3) "C-bound" CO in an all "C-bound" monolayer on NaCl(100) (model B) are pre-excited by ~ 26 and ~ 14 vibrational quanta, respectively (0.26 eV). These quantities for case (2) provide a complementary understanding of the reported transient VSF response of the CO stretch mode in the main text (Sec. 3.3.2). Further, averaged angular probability distributions before and after inducing the non-equilibrium conditions are reported for the same scenario (2).

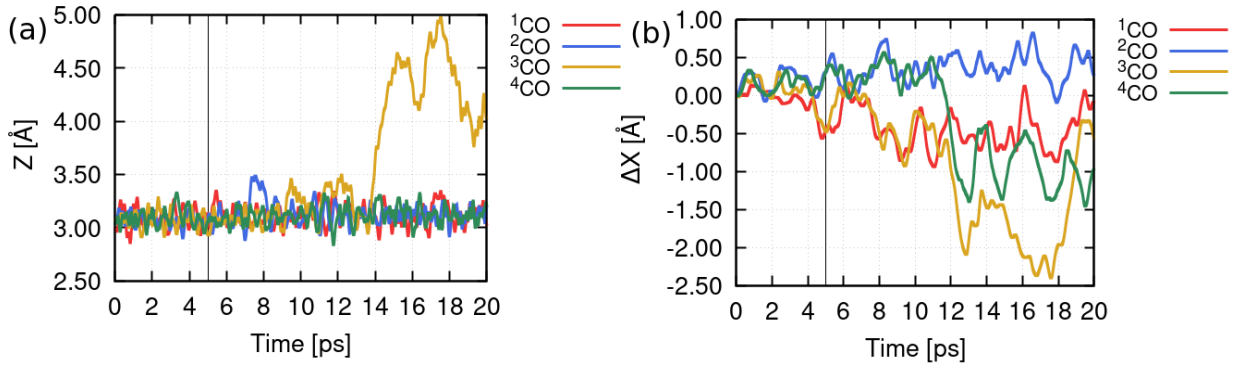

Figure S14: Average CO-surface (Z) (a), and lateral displacements w.r.t. initial times (ΔX) (b), for all CO adsorbates, when ^{1}CO is pre-excited by one vibrational stretch quantum in an all "O-bound" configuration (case (1) of above)). One notes roaming dynamics during CO flipping in more than one adsorbate along with near desorption of the one of the CO molecules after 9 ps of pre-excitation. Pre-excitation occurs at 5 ps (vertical lines).

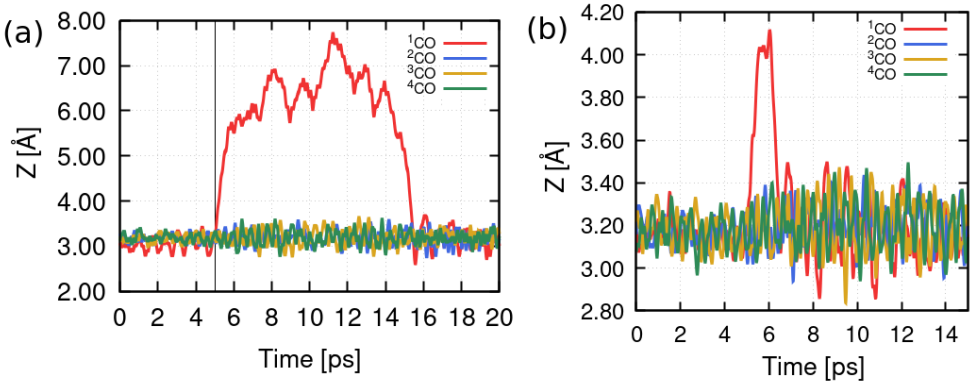

Figure S15: One instance of roaming trajectory observed for the flipping of (a) "O-bound" CO molecule (^{1}CO) (case (2) of above), of (b) "C-bound" CO molecule (^{1}CO) (case (3) of above), when the frustrated bending mode is pre-excited by 26 and 14 vibrational quanta, respectively.

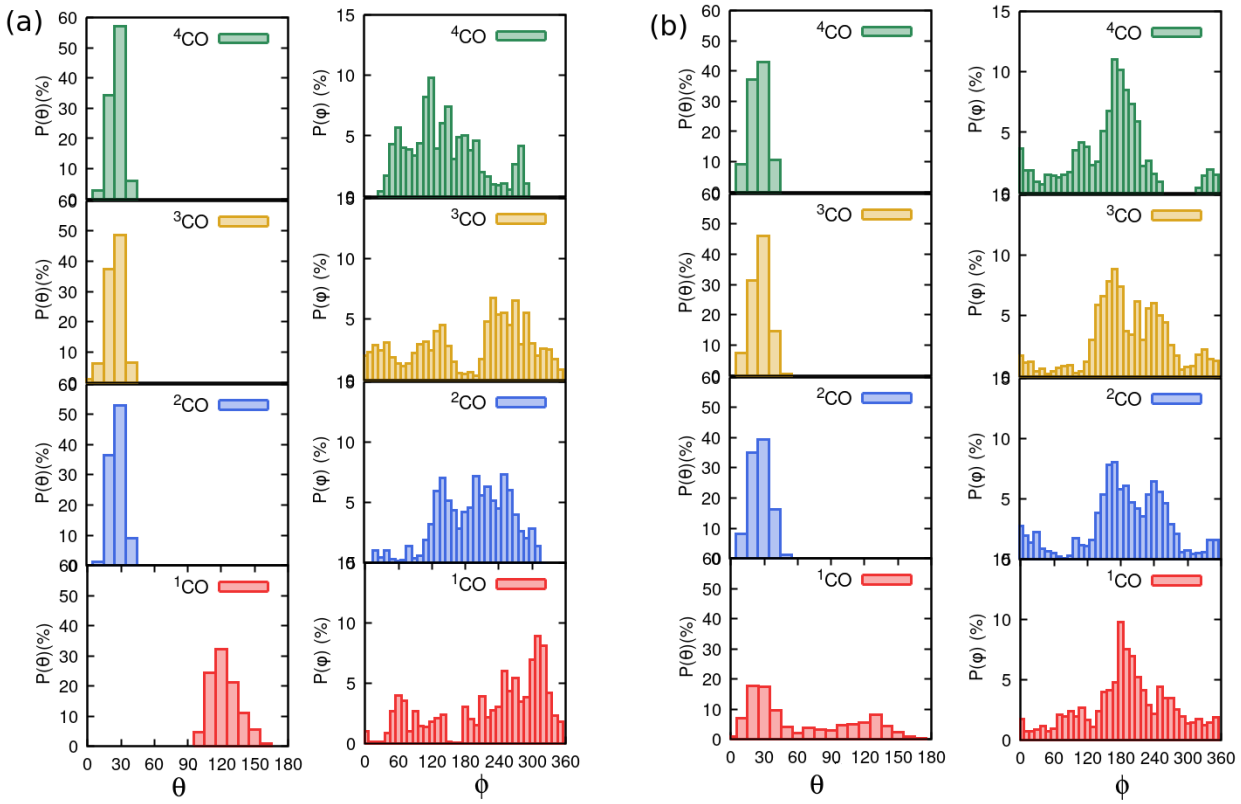

Figure S16: Probability distribution curves of angular DoFs (θ, ϕ) (a) before and (b) after pre-excitation of the frustrated bending mode of an "O-bound" CO in a monolayer one "O-bound" CO/NaCl(100), by 26 vibrational quanta of the respective mode (case (2) of above).

S11 Non-equilibrium dynamics with NN potentials

In addition to the ns dynamics based on a NN potential for CO/NaCl(100)[4] provided in the main text, Sec. 3.1.3, we report here an instance of relaxation dynamics for a 150 ps long trajectory for a relaxing "O-down" CO in a one "O-bound" monolayer (model C), post pre-excitation of a frustrated bending mode by $\sim$ 26 quanta (0.26 eV). We find similar short-timescale dynamics, dominated by isomerization, roaming events and a predominant transfer of energy to the NaCl surface as before, on shorter timescales. We also observe, however, from Fig. S17 that around 120 ps, there is a backward flux of energy from the "vibrationally hot" surface to the CO adsorbate(s) over a period of 10 ps, which is regained back by the phonons in another 10 ps.

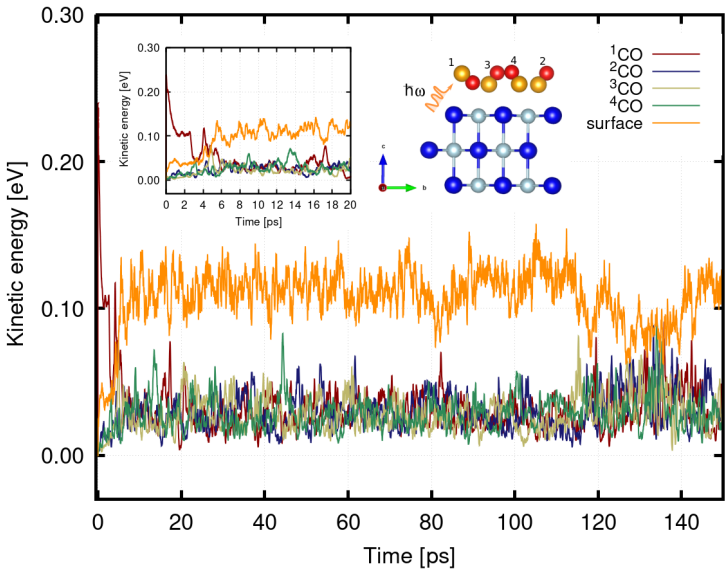

Figure S17: a) Averaged trendlines[1]of instantaneous kinetic energies decomposed into sub-systems, for a non-equilibrium trajectory of 150 ps, after pre-excitation of one of the CO adsorbates (^{1}CO) by 26 vibrational quanta ($\sim$ 0.26 eV) in a frustrated bending mode.

[1]A moving average trendline calculates the average of a specific number of data points over equal intervals (in this case, a period of 0.25 fs) and plots these averages as points on the trendline. This approach reduces data fluctuations and enhances visualization by smoothing the data.

References

(1) Sinha, S.; Wodtke, A. M.; Saalfrank, P. When carbon monoxide goes "upside down": vibrational signatures of CO at NaCl(100) from ab initio molecular dynamics. *Phys. Chem. Chem. Phys.* **2025**, *27*, 7929–7942.

(2) Jeon, J.; Hsieh, C.-S.; Nagata, Y.; Bonn, M.; Cho, M. Hydrogen bonding and vibrational energy relaxation of interfacial water: A full DFT molecular dynamics simulation. *The Journal of Chemical Physics* **2017**, *147*, 044707.

(3) Melani, G.; Nagata, Y.; Saalfrank, P. Vibrational energy relaxation of interfacial OH on a water-covered -Al2O3(0001) surface: a non-equilibrium ab initio molecular dynamics study. *Phys. Chem. Chem. Phys.* **2021**, *23*, 7714–7723.

(4) Sinha, S.; Mladineo, B.; Lončarić, I.; Saalfrank, P. Multidimensional Neural Network Interatomic Potentials for CO on NaCl(100). *The Journal of Physical Chemistry C* **2024**, *128*, 21117–21131.